

**FULL PAPER****Applied
Organometallic
Chemistry****WILEY**

Blue Highly Fluorescent Boranil Derived From Anil Ligand: Synthesis, Characterization, Experimental and Theoretical Evaluation of Solvent Effect on Structures and Photophysical Properties

Soumaya Agren¹ | Marwa Chaabene² | Abdul-Rahman Allouche³ | Rafik Ben Chaâbane² | Mohamed Lahcinie^{4,5} | Mohamed Hassen V Baouab¹

¹Research Unit Materials and Organic Synthesis (UR17ES31), Preparatory Institute for Engineering Studies of Monastir, University of Monastir, Avenue of the Environment, Monastir, 5000, Tunisia

²Laboratory of Advanced Materials and Interfaces (LIMA), Faculty of Sciences of Monastir, University of Monastir, Avenue of the Environment, Monastir, 5000, Tunisia

³Institute of Light and Matter, UMR5306 University of Lyon 1-CNRS, University of Lyon, cedex, Villeurbanne, 69622, France

⁴Laboratory of organometallic and macromolecular chemistry-composites Materials, Faculty of Sciences and Technologies, Cadi Ayyad University, Avenue Abdelhakim Elkhattabi, BP549, Marrakech, 40000, Morocco

⁵Mohamed VI Polytechnic University, Lot 660, Hay Moulay Rachid, Ben Guerir, 43150, Morocco

Correspondence

Mohamed Hassen V Baouab, Research Unit Materials and Organic Synthesis (UR17ES31), Preparatory Institute for Engineering Studies of Monastir, University of Monastir, Avenue de l'Environnement 5019 Monastir Tunisie. Email: hbaouab@yahoo.fr

Funding information

Tunisia-Morocco, Grant/Award Number: N°17/TM10

In this study, we report the design and the synthesis of a Schiff base; Anil and its corresponding Boron Difluoride complexe; Boranil. The synthesis procedure was carried out adopting new, optimized reaction conditions. The Boranil dye presents the advantage to be emissive in solution. ¹H and ¹⁹F NMR along with FTIR confirmed both compound's structure. To gain a better understanding of the solvatochromic behavior of Anil and Boranil, the dependence of the absorption spectra on the solvent's polarity was studied in depth. Thus, UV-Vis spectroscopy was performed in five selected solvents. In addition to the solvent's polarity effect, the influence of BF₂ moiety introduction on the molecule's photophysical properties was also evaluated. When examining different absorption spectra, we found that the title fluorescent dye exhibited weak solvatochromic (11 nm in THF) as well as a slight redshift broader and relatively more structured absorption spectra after complexation. Besides, we investigate the obtained key structure–property relationships through DFT and TD-DFT calculations using a 6-311++G(d, p) basis set. Quantum chemical calculations allowed confirming proposed structures and understanding their electronic structure in larger details. Theoretical results also showed good agreement with the experimental findings. Finally, the frontier molecular orbitals were investigated to illustrate the pi-conjugation and charge transfer effect.

KEY WORDS

Anil, Boranil, FTIR, HOMO-LUMO analysis, solvent effect

1 | INTRODUCTION

Nowadays, organic fluorescent dyes are considered as potential materials due to their multidisciplinary applications in different fields including Bioimaging^[1,2], Organic light-emitting diodes (OLED),^[3–5] dye-sensitized solar cells (DSSC),^[6] chemosensors,^[7] medicinal and pharmaceutical applications such as saccharides sensing^[8] and explosives detection.^[9] The use of N, O, π conjugated ligands heterocyclic coordination center has opened the way to obtain various new families of fluorescent dyes. The extent of the π-bond conjugated system of these chromophores is responsible for their remarkable fluorescent color. Notably, Tetracoordinate Organic Boron Difluoride Complexes are known to be fluorescent.^[10] The study of different Boron Difluoride organic complexes has been the subject of great research interest.^[11–16] In this context, researchers are focusing on developing new materials with desired properties through simple synthetic procedures and low cost. Particularly, Boranils show excellent properties such as essentially broad and structured absorption bands.^[11,13–16] These molecules can be used as potential alternative candidates to the most studied known fluorescent compounds Bodipys^[17,18] that have received overwhelming interest because of their outstanding optical properties.^[19] Several studies highlighted their exceptional chemical stability and promising spectroscopic features.^[17–20]

To date, the study of these systems has been focused on substituted Schiff bases and their corresponding Boranils due to their high stability.^[11,14,21–23] Moreover, It has been proved that the stability of the B-N and B-O bonds is critical for maintaining desired optical properties.^[23] Furthermore, Rao and coworkers emphasize that the key role of boron is stabilizing the anionic chelating (NO) ligand.^[24] To improve the boranil complexes' stability, Frath and coworkers suggested a push-pull system. The proposed system can enhance the dye's emission without any disruption of the boron chelate ring.^[22] Additionally, Frath and co-workers outlined also their strategy to achieve with success the synthesis of the first series of polyanils and their corresponding luminescent polyboranils. These polyboranils were also functionalized by sterically hindered substituents to enhance their solid-state emission.^[12] Recently, we have successfully investigated the photophysical and optoelectronic properties of Boron Difluoride fluorescent dyes and their corresponding ligands through a completely experimental and theoretical study in DMF solvent.^[25] Bearing in mind all the above considerations, we have decided to broaden our work and face all these difficulties to obtain a Boron Difluoride complexe with a moderate yield. We

have optimized the different reaction conditions. Our synthetic approach is based on extending the reaction time and modifying other reaction parameters such as the non-bulky Base and the dried Toluen solvent through distillation. The Boranil (b) is synthesized for the first time from the unsubstituted Anil (a) known in recent studies as salicylideneaniline.^[26,27] This compound exhibits upon excitation an extremely ultrafast intermolecular proton transfer from the hydroxyl group to the nitrogen atom.^[26] This ESIPT phenomenon leads to a cис-keto form, which is quickly converted into a photochromic product. In addition to ultrafast ESIPT phenomenon, these compounds exhibit several non-radiative deexcitation channels competing with the mentioned above phenomena such as twisting about CN and CC bonds, π-π* to n-π* internal conversion and singlet-triplet inter system crossing.^[26] This would allow us to address one of the most important challenges regarding the unsubstituted ligand system. A substituted Anil seems to have better stability and easier Boron Difluoride complexation.^[12,26] $\text{BF}_3\text{Et}_2\text{O}$ acts usually as the main source of the boron in the preparation of π conjugated boron complexes.^[28]

This contribution aims to develop a new improved synthetic procedure of an unsubstituted Boranil as well as a detailed characterization of the target compounds using ^1H and ^{19}F NMR along with FTIR. We compared the media polarity's effect on chemical stability and photophysical properties. We have figured out that the solvent effect can also be exploited for tuning their optical properties. DFT and TD-DFT calculations have been carried out to elucidate the influence of the structural modification and solvent polarity on the spectroscopic and electronic properties as well as providing insights into the factors controlling charge transfer phenomenon.

2 | EXPERIMENTAL SECTION

2.1 | Materials and methods

^1H and ^{19}F NMR spectra were measured by Bruker 300 MHz NMR spectrometer. FTIR spectra were measured on a Perkin Elmer spectrum ranging from 350 to 8300 cm^{-1} with DTGS as a detector. UV-vis absorption spectra were obtained on a SPECORD PLUS ranging from 190–1100 nm.

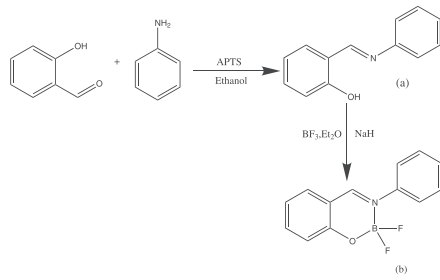
2.2 | Quantum chemical calculation

The molecular structure of the synthesized compounds in the ground state has been optimized by the DFT method

using B3LYP functional with the empirical dispersion correction D3 of Grimme et al.^[29] 6-311++G (d, p) basis set with diffuse functions has been used for all calculations.^[30,31] ¹H-NMR shielding constants have been calculated by applying the gauge-invariant atomic orbital (GIAO) method.^[32,33] Frequency calculations of all compounds have also been performed to confirm the location of the optimized structures at the local minima with the same basis in the gas phase. The energy gap (Eg) between the highest occupied molecular orbital (HOMO) and the lowest unoccupied molecular orbital (LUMO) has been calculated for all compounds in different solvents. Also, contribution percentages of the excitations were calculated using GaussSum 3.0 program.^[34] Besides, simulated absorption spectra of all synthesized molecules in different solvents have been performed at the time-dependent density functional theory (TD-DFT) using theCAM-B3LYP level.^[35,36] All optoelectronic calculations were performed using the Gaussian09 program^[37] and visualizations were carried by the graphical interfaces Gabedit^[38] and Gaussview.^[39]

2.3 | Synthesis procedure

As summarized in Scheme 1, the Anil (a): (E)2((phenylimino)methyl) phenol has been prepared in good yield by refluxing the 1:1 molecular ratio of aniline and salicylaldehyde in absolute ethanol and in the presence of trace amounts of p-TsOH. After heating the solution at reflux for 24 hr, the Anil (a) precipitates pure out of the reaction mixture and can be purified by filtration after cooling the mixture to room temperature. Afterward, obtained yellow crystals have been collected and air-dried. Subsequent Boron (III) complexation has been achieved for six days in dry toluene with BF₃.Et₂O (BF₂) under basic conditions and N₂ atmosphere to form Boranil (b). The desired Boranil was obtained as a brown oil and was extracted with acetyl acetate. After solvent removal, the crude product has been purified by column



SCHEME 1 General scheme for the synthesis of Anil and its corresponding Boranil

chromatography (silica gel, CH₂Cl₂/Petroleum Ether, v/v = 4/6).

3 | RESULTS AND DISCUSSION

3.1 | Geometric structure

The DFT/B3LYP-D3 optimized geometries at 6-311++G (d, p) level of Anil (a) and Boranil (b), in THF solvent is shown in Figure 1. We have chosen this solvent because it gives the highest total energy compared to the other solvents. Therefore, the two molecules (a) and (b) are more stable in THF (see Table 4) than in other solvents. The selected computational values of bond lengths and bond angles are given below in Table 1. Overall, the generation of BF₂ six-membered ring slightly modifies the geometric structure of the Anil compound and can make a great contribution to the rigidity of the Anil (a) structure. This improved structural rigidity is one of the most significant reasons for its intensive fluorescence.^[40] Notably, both dyes have an almost planar structure and Anil's complexation slightly affects all common bond lengths. It also appears that the B₂₅-O₂₄ and N₂₁-B₂₅ bond lengths are respectively 1.464 Å and 1.606 Å, which is in agreement with those reported for analogous six-membered ring BF₂ complexes.^[21,41,42] The bond angles between (C₁₂-C₁₁-C₂₂) of the BF₂ six-membered ring plane has a relatively considerable twist than those of Anil (a). Those changes can essentially be in the reflection of the electronegativity of the Fluorine atoms.^[21]

3.2 | NMR Spectrum analysis

To confirm elemental composition and purity, ¹H and ¹⁹F NMR spectral data of both synthesized compounds (a) and (b) have been recorded in deuterated DMSO at 300 MHz spectrometer and room temperature.

The assignment of each proton's resonance should be based on its integration and multiplicity pattern. However, a detailed proton's assignment is not possible due to the strong π electron delocalization of aromatic protons.

Anil (a); δ = 12.12 (s, 1H, OH), 9.12 (s, 1H, CH=N), 6.98–7.38 (m, 3H), 7.07–7.44 (dd, J = 2.410 Hz, 2H), 7.66 (dd, J = 2.781 Hz, 2H), 7.52 (dd, J = 1.221 Hz, 2H).

Boranil (b); δ = 8.4 (s, 1H, CH=N), 6.96–6.99 (dd, J = 1.97, 3H), 7.07–7.44 (dd, J = 1.28 Hz, 2H), 7.52 (td, J = 2.348 Hz, 3H), 7.52 (m, 2H).

The GIAO ¹H chemical shift calculation of (a) and (b) are simulated at B3LYP-D3/6-311++G (d, p) and

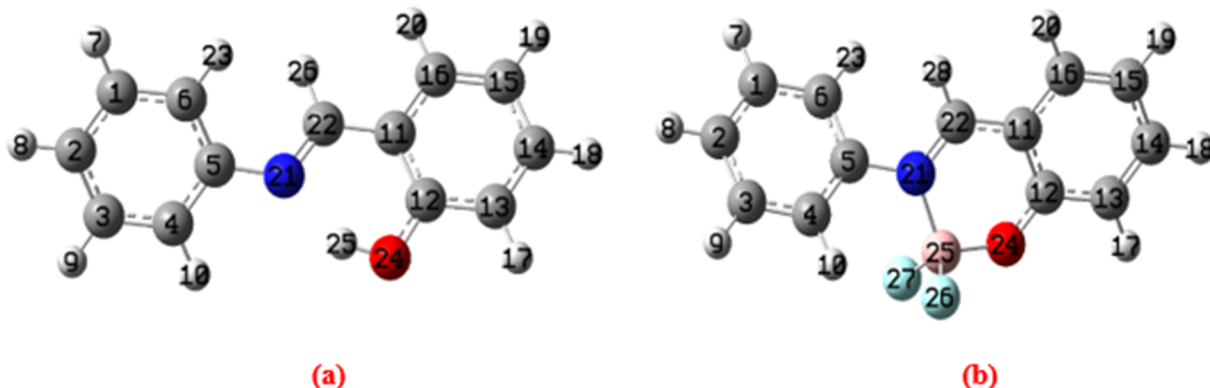


FIGURE 1 Optimized structures of (a) and (b) calculated at B3LYP-D3/6-311++G (d, p)

TABLE 1 The calculation bond length (in Å) and bond angles (°) of (a) and (b) by DFT at 6-311++G (d, p) basis set level

Parametres	(a)	(b)
Bond length (Å)		
O ₂₄ -C ₁₂	1.344	1.323
C ₁₂ -C ₁₁	1.421	1.419
C ₁₁ -C ₂₂	1.449	1.423
C ₂₂ -H ₂₆ for (a)	1.096	1.087
C ₂₂ -H ₂₈ for (b)		
C ₂₂ -N ₂₁	1.288	1.304
N ₂₁ -C ₅	1.408	1.433
F ₂₆ -B ₂₅	----	1.401
F ₂₇ -B ₂₅	----	1.382
B ₂₅ -O ₂₄	----	1.464
N ₂₁ -B ₂₅	----	1.606
Bond angle (°)		
O ₂₄ -C ₂₁ -C ₁₁	122	121
C ₁₂ -C ₁₁ -C ₂₂	121	118
C ₁₁ -C ₂₂ -N ₂₁	122	122
C ₂₂ -N ₂₁ -C ₅	121	120
H ₂₅ -O ₂₄ -C ₁₂	107	----
B ₂₅ -O ₂₄ -C ₁₂	----	123
C ₂₂ -N ₂₁ -B ₂₅	----	120
N ₂₁ -B ₂₅ -O ₂₄	----	109

compared to the experimental data. As a general overview, ^1H and ^{19}F NMR values have been in excellent agreement with both proposed structures (see Table 2) and both studied compounds yield similar proton spectra except for the disappearance of hydroxyl proton for (b) spectrum. ^1H NMR spectra of (a) and (b) exhibits the typical aromatic protons multiple and a typical imine proton $\text{N}=\text{CH}$ signal. A careful examination of proton

shifts among the Boranil spectrum reveals a downward shift in all proton signals. The imine proton shifts to lower field proving the success of B-N bond formation and the participation of the nitrogen atom in Boron coordination.^[43] All obtained results are in agreement with data reported for similar Schiff bases and their corresponding Boranils.^[44-46] Further evidence for the identity of the Boranil compound comes from ¹⁹F NMR spectral data. ¹⁹F NMR spectrum exhibits a well-resolved doublet broad signals at $\delta = -148.41$ and -148.34 ppm revealing the presence of two non-equivalent Fluorine atoms split by a Boron atom. The absence of quartets in the ¹⁹F NMR spectra is occasionally explained to be the result of the fast relaxation of the quadrupolar boron nuclei.^[47] Doušová and co-workers reported that this behavior could be the result of an additional not observed splitting into doublets (due to the geminal 19F-19F coupling). This phenomenon can occur in the case of the non-equivalence of the fluorines at room temperature.^[47] The substitution does not affect ¹⁹F NMR spectra and resonances are practically the same as mentioned in our recent work.^[25] Slight differences between experimental and theoretical values are essentially due to the model used to be taken into account of the solvent effect on the molecule. The PCM, used here, is not able to predict the local strong interaction between liquid and the molecule.^[25]

3.3 | IR Spectrum analysis

A survey of the literature reveals that the FTIR spectroscopy has been proven useful in confirming the proposed structures of Anils, Boranils and similar organic compounds.^[12,26,48,49] We have performed frequency calculations using B3LYP-D3/6-311++G (d, p) basis set in the gas phase. The simulated harmonic vibrational

TABLE 2 Experimental and theoretical calculation NMR of ^1H and ^{19}F for (b)

(a)	δ_{exp} (ppm)	δ_{theo} (ppm)
H ₇	7.07	7.79
H ₈	7.47	7.61
H ₉	7.44	7.77
H ₁₀	7.52	7.69
H ₁₇	6.98	7.27
H ₁₈	7.38	7.69
H ₁₉	7.16	7.20
H ₂₀	7.66	7.77
H ₂₃	7.47	7.55
H ₂₅	12.12	12.93
H ₂₆	9.12	9.32
(b)	δ_{exp} (ppm)	δ_{theo} (ppm)
H ₇	6.96	7.90
H ₈	7.18	7.86
H ₉	6.99	7.8
H ₁₀	7.96	8.32
H ₁₇	7.68	7.75
H ₁₈	6.95	8
H ₁₉	7.52	7.64
H ₂₀	7.49	7.87
H ₂₃	7.02	7.56
H ₂₈	8.4	8.55
F ₂₆	-148.35	---
F ₂₇	-148.40	---

wavenumbers have been scaled down uniformly by a factor of 0.987 (for wavenumbers under 1800 cm^{-1}) and 0.961 (for those over 1800 cm^{-1}), which accounts for systematic errors caused by basis set incompleteness, neglect of vibrational anharmonicity and electron correlation.^[50] The observed wavenumbers computed unscaled and scaled frequencies of all studied compounds are listed in Table 3. The experimental and computed FTIR of the title compounds are presented in Figure 2.

Both studied compounds have been characterized by infrared spectroscopy where they exhibit typical peaks with the appropriate shifts resulting from bonds formation. Organoboron Difluoride complex is compared to its Anil ligand in order to investigate the coordination possible sites that could be involved in chelation. Depending on their molecular structure, both studied compounds display C-H and C=C stretching and bending vibrations. Those vibrations are extremely informative and are very convenient for characterization purposes.^[12] All obtained

vibration modes, for both molecules (a) and (b), are very close to those resulting from our previous study where we have investigated and discussed in detail all vibration modes.^[25] Generally, the CH out of plane bending vibrations in aromatic compounds occur between 700 cm^{-1} and 1000 cm^{-1} .^[51] It is well known that CH out of plane deformation presenting higher frequencies has a weaker intensity than those absorbing at lower frequencies.^[52] Therefore, The assignments of peaks in the region of the corresponding region were not easy and this region was dominated by very massive bands.

In the present work, All studied compounds exhibit relatively weak absorption peaks in the region of 690 – 780 cm^{-1} , 675 – 822 cm^{-1} respectively for (a) and (b) respectively and are assigned to CH out of plane bending vibrational modes. These results show that complexation has an obvious influence on their values and show good agreement with the theoretical results (see Table 3).

In addition, the CH in-plane deformation vibrations for substituted benzenes are seen in the range of 1000 – 1300 cm^{-1} .

Several in-plane bending vibrations of the studied Anil (a) and its Boranil (b) are identified in the range of 1073 – 1614 cm^{-1} and 1000 – 1662 cm^{-1} respectively. The theoretically calculated values appear in the range of 1171 – 1644 cm^{-1} , 1025 – 1646 cm^{-1} for (a) and (b) respectively, which shows that the predicted values are coinciding very well with the observed frequencies. Taking into account the structure modification through Boron Difluoride complexation, there is not an appreciable influence on the in-plane bending vibrations of the studied Boranil (b).

Furthermore, in the context of the results of the previous study, the recently studied Anil^[25] spectra display peaks in the range of 1400 – 1660 cm^{-1} due to the azomethine C=N peaks for studied Anils and Boranils. The computed values of these compounds are observed at 1471 , 1586 and 1610 cm^{-1} for (a) which implies good agreement with the experimental findings. Peaks corresponding to C=N stretching vibrations in the investigated Boranil (b) shift to higher wavenumber which indicates that the coordination takes place through nitrogen atoms of azomethine groups.^[25] The ring stretching vibrations are extreme characteristics of the aromatic rings^[48] and their derivatives.^[53]

Most of the aromatic compounds undergo coupled vibrations called skeletal vibrations^[48] in the region of 1100 – 1600 cm^{-1} due to C-C and C=C stretching peaks.^[25] In the same line of thought and in the presence of the findings of an earlier study,^[25] (a) and (b) exhibit C-C and C=C stretching peaks (see Table 3) which are very well within the cited literature range and show that

TABLE 3 Experimental and theoretical vibrational frequencies (cm^{-1}) of Anil (a) and its corresponding Boranil (b)

(a)			(b)		
ν_{calc} Unscaled	ν_{calc} Scaled	ν_{Exp}	Vibration*	ν_{calc} Unscaled	ν_{calc} Scaled
				ν_{Exp}	Vibration*
705	696	690	CH oopb	708	699
763	753	751	CH s oopb	765	755
849	838	780	CH oopb+ OH tors	861	850
1108	1093	1073	CH ipb + CC str	1039	1025
1186	1171	1149	CH ipb	1160	1145
1214	1198	1185	CH ipb + OH b + CC str	1229	1213
1315	1297	1276	CO str + CC str + CH ipb	1353	1335
1449	1430	1401	CHipr+ OH b	1416	1398
1490	1471	1453	CH ipb + CC str + CO str + OH b	1510	1490
1607	1586	1568	CH ipb + OH b + CNstr+ CC str	1579	1558
1631	1610	1588	CHipb+ CC str + CN str + OH b + CO str	1632	1610
1666	1644	1614	CH ipb + CC str + CN str + CO str	1668	1646
3031–3185	2913–3061	2828–3040	CHstr+ OH str	3139–3350	3016–3219
3215	3090	3077	OH str	---	---
				2823–3501	CH str

s: symmetric; as: asymmetric; str: stretching; r: rocking; b: bending; oop: out of plane; ipb: in plane bending; tors: torsion; r: rocking.

*The majority of harmonic modes were composed of a variety of local modes. Only the local modes that have the most important contribution were listed in the Table.

^aObtained from the wave numbers calculated at B3LYP-D3(6-311++G(d,p) using scaling factors 0.987 (for wave numbers under 1800 cm^{-1}) and 0.961 (for those over 1800 cm^{-1}).

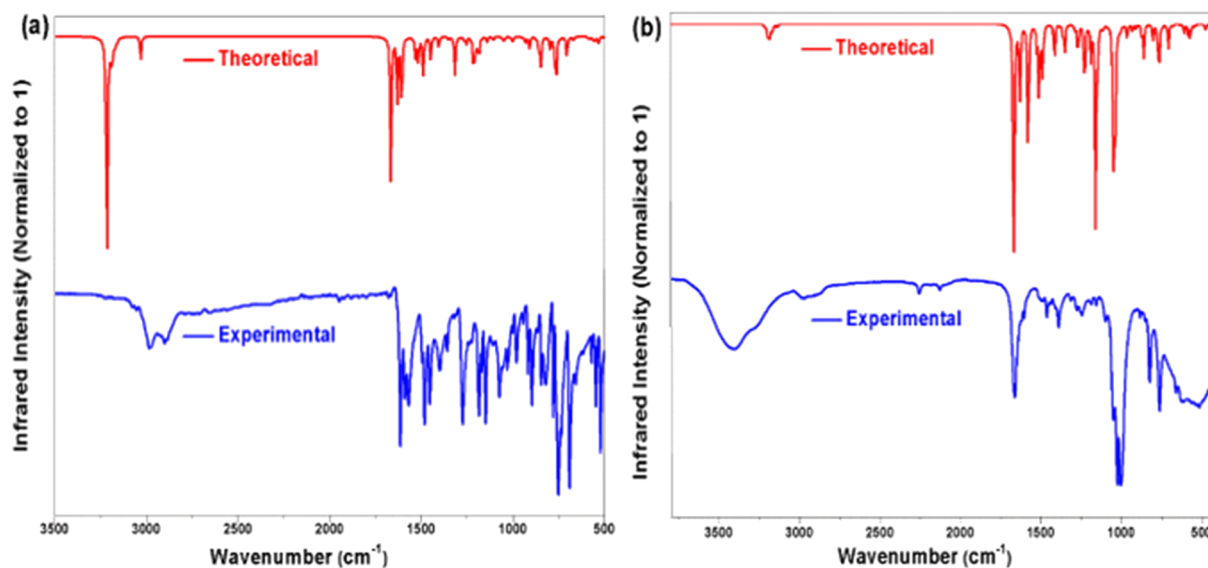


FIGURE 2 Comparison of experimental and theoretical FT-IR spectra for (a) and (b)

the ring skeletal vibrations remain independent of other vibration in the molecule.^[53]

It is important to emphasize that the complexation upfield CO stretching vibrations from 1453 cm^{-1} for (a) to 1460 cm^{-1} for (b). This trend is observed in our recent study.^[25] We note also the appearance of novel peaks in the range of $822\text{--}1662\text{ cm}^{-1}$ for (b). Those results are similar to those obtained for a similar molecule in our recent study ($883\text{--}1093\text{ cm}^{-1}$)^[25] corresponding for B-N, B-O and B-F bending peaks. These results strongly support the formation of foregoing Organoboron Difluoride Complexes.^[11] According to a detailed study reported by 14,^[14] the appearance of a strong stretching vibration above 1060 cm^{-1} may be essentially due to B-N vibration mode. Moreover, peaks in the region of 880 cm^{-1} ^[25] were attributed to B-F stretching vibrations. Also, The existence of B-O bond is proven by the disappearance of O-H bond.^[25]

For aromatic rings, CH stretching vibrations are expected to occur above 3000 cm^{-1} . Peaks observed in the range of $2823\text{--}3040\text{ cm}^{-1}$ and $2823\text{--}3501\text{ cm}^{-1}$ are respectively assigned for CH stretching vibrations of (a) and (b). In the light of these results, we clearly notice that complexation using BF_3 , Et_2O upfield CH stretching vibrations. For the hydroxyl group, all the preceding^[25] and actual spectra prove that OH stretching vibrations are sensitive to hydrogen bonding^[52] and are predicted in the range of 3500 cm^{-1} . For the title compound (a), a weak and broad peak appears in the range of $2828\text{--}3070\text{ cm}^{-1}$ and is interpreted to be a sign of the formation of hydrogen bonding.^[45] This peak disappears in organoboron difluoride complexe spectra indicting deprotonation of ligands through Boron coordination.

As shown in Table 3, the comparison of the scaled calculated frequencies gives reasonable deviations from the experimental values.

3.4 | Photophysical properties

3.4.1 | Frontier molecular orbital analysis

The electronic and quantum chemical properties of the optimized structure of (a) and (b) in different solvents are listed in Table 4. The energy gap between HOMO and LUMO is a critical parameter property for quantum chemistry.^[54] It determines the chemical activity and the kinetic stability of the molecules^[55] based on DFT calculations. From the results shown in Table 4, we can deduce that the energy band gap of (a) has decreased after the complexation with BF_2 in all solvents. The compounds (a) and (b) in the gas and the cyclohexane solvent have the lowest gap energy compared to other solvents. The electronic chemical potential (μ) is a chemical property that describes the ability of an atom or a functional group to attract electrons or electron density towards itself.^[56] The chemical hardness (η) measures both the stability and the reactivity of a molecule.^[57] The global softness (σ) describes the capacity of an atom or group of atoms to receive electrons. The values of (μ) and (σ) have increased after the complexation with BF_2 whereas the values of (η) are decreased after the addition of BF_2 as shown in Table 4.

To establish a logical correlation, we may conclude that the addition of BF_2 makes the molecule (b) more conductive and more polarizable (with lower molecular

TABLE 4 The calculated electronic and quantum chemical parameters for (a) and (b) different solvents at DFT/B3LYP-D3/6-311++G (d, p)

	solvents	HOMO	LUMO	Eg	μ (eV)	η (eV)	σ (eV ⁻¹)	μ_D (D)	E _T (a.u)
(a)	Chloroform	-6.296	-2.119	4.177	4.208	2.089	0.479	3.089	-632.179222
	Cyclohexan	-6.261	-2.096	4.165	4.179	2.082	0.480	2.722	-632.176845
	THF	-6.311	-2.129	4.182	4.220	2.091	0.478	3.227	-632.180062
	Toluen	-6.269	-2.100	4.169	4.184	2.084	0.480	2.803	-632.177386
	Gas	-6.232	-2.086	4.146	4.159	2.073	0.482	2.346	-632.174162
(b)	Chloroform	-6.752	-2.775	3.977	4.763	1.989	0.503	7.899	-856.381410
	Cyclohexan	-6.724	-2.782	3.942	4.753	1.971	0.507	6.974	-856.376055
	THF	-6.764	-2.773	3.991	4.768	1.996	0.501	8.245	-856.383294
	Toluen	-6.730	-2.780	3.950	4.755	1.975	0.506	7.179	-856.377281
	Gas	-6.703	-2.798	3.905	4.751	1.953	0.512	6.011	-856.369890

$$Eg \approx E_{LUMO} - E_{HOMO}$$

$$\mu = -[E_{HOMO} + E_{LUMO}] / 2$$

$$\eta = [E_{LUMO} - E_{HOMO}] / 2$$

$$\sigma = 1/\eta$$

stability and high reactivity in chemical reactions) compared to its Anil (a) especially in the gas phase and the cyclohexane solvent. However, (a) and (b) are harder and more stabilized using THF and chloroform solvents than in other solvents.

The contour plots of HOMO and LUMO investigated at the DFT/B3LYP-D3/6-311++G (d, p) level of all compounds are shown in Figure 3 in cyclohexane solvent. The electronic absorption properties are explained from the frontier molecular orbitals (HOMO and LUMO).^[58] The positive phase is presented in red

color and the negative one is in green. It can be deduced from this figure that the electron density of HOMO is mostly identically localized on both phenyl rings and azomethine moiety of (a) and their π -bonding orbitals. Similarly, we get analogous results for (b). Whereas, The LUMO electronic distribution mainly populate on one phenyl ring than another especially after complexation and also their π^* -bonding orbitals. Owing to the extent of π conjugation after the introduction of BF₂ moiety, these results suggest that structural modification has a significant effect on the

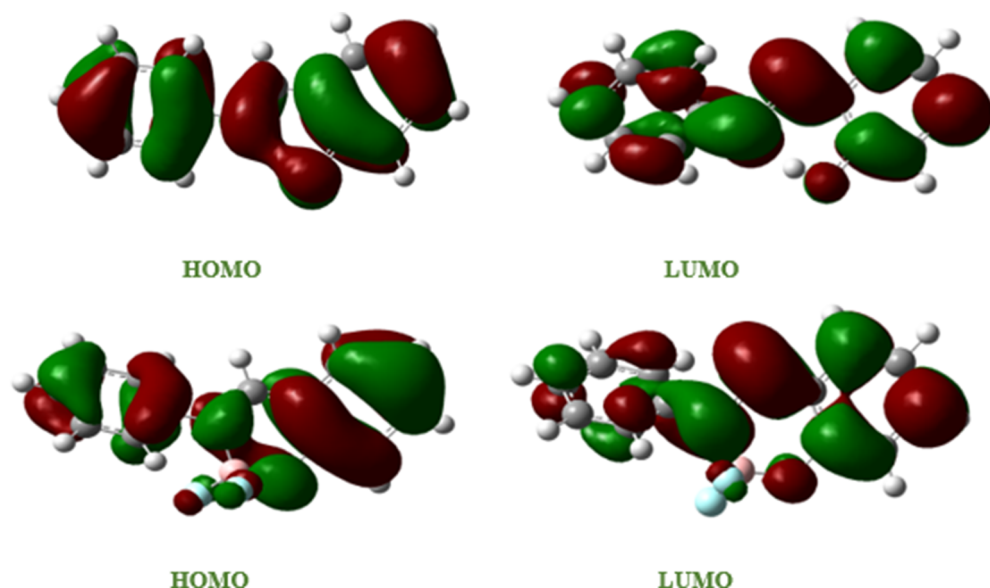


FIGURE 3 The frontier molecular orbitals of (a) and (b)

electronic density distribution. These differences can explain the different observed emission behavior.

3.4.2 | Electronic absorption spectra

In order to investigate the photophysical properties of the studied anil and its Boron Difluoride Complex; Boranil. UV-vis absorption measurements are carried out experimentally as well as theoretically using four different solvents at room temperature: non-polar aprotic solvents (cyclohexan, toluen and chloroform). Polar aprotic solvent (THF) is selected and the concentration of each solution sample is maintained to be 10–4 M. TD-DFT calculations on electronic absorption spectra in the previous solvents and in the gas phase were performed. The calculations have been carried out using the CAM-B3LYP/6-311++G (d, p) method. The absorption wavelengths (λ max), oscillator strengths (f) and major and minor contributions (%) of (a) and (b) for solvents and gas phase are illustrated in Table 5.

As a general observation, Boron Difluoride complexe: Boranil shows good solubility and has a blue light emission under UV light in all tested organic media such as Cyclohexane, toluene, chloroform, and THF. By testing, no observable color and fluorescence fading has been noticed over months.

It is apparent that there is a qualitative correlation between the optical properties and the molecular structures. The combined effect of solvent polarity and complexation is evident and has been widely studied.^[16,59]

Solvent effects can be explained with the capacity of hydrogen bonding both as proton donors and as proton acceptors, thus permitting the proton transfers that result in the formation of the keto form of the studied Anil (a). The solvent interacts with the non-bonding electron pair of the azomethine nitrogen.^[45] As a result, specific solute-solvent interactions can lead to a qualitative and quantitative change in the Anil spectra (Figure 4). According to literature, Solvent effects are relevant in Anils tautomers stability phenomena, since polarity differences among tautomers can induce significant changes in their relative energies in solution.^[60] Besides, the excited state of any donor-acceptor compound such as Boranil gets strongly affected by solvents polarity due to its stabilization through dipole-dipole, hydrogen bonding and solvation interactions.^[61]

Both studied compounds have shown remarkable solvatochromism behavior.^[20] Using different solvents has an obvious effect on the intensity and the broadness of studied Anil and Boranil spectra. A direct comparison of the photophysical properties reveals that an increase in solvent polarity doesn't have a relative

effect on the short wavelengths absorption band's intensity Long wavelengths absorption bands seem to be dependent on the dipole moment of the solvent and their intensities vary according to solvent polarity after complexation as shown in Figure 4. Therefore, the short wavelengths will not be taken as references for the Anil and Boranil spectra analysis. An increase in solvent polarity causes a bathochromic shift^[61] for Anil spectra in the long-wavelength absorption bands. This assumption demonstrates that the media polarity affects essentially the keto forms rather than the enol ones; it destabilizes the singlet excited state and/or stabilizes the ground state of the keto forms.^[62] Thus, Stabilizing the ground state is a direct cause of the non-fluorescence of (a).

Figure 4 represents comparative experimental and theoretical absorption spectra of the studied Anil (a) in different solvents. As a general trend, all Anil absorption spectra display generally almost similar absorption spectra; a large, unstructured absorption band located around 300–490 nm. The absence of structuration of the absorption bands is probably related to free rotations occurring in solution as reported in a previous study.^[63] Bands observed at short wavelengths may be attributed to electronic transitions from low lying molecular orbitals to the LUMO. This phenomenon could also be caused by the limited donor acceptor charge transfer due to the small extent of the conjugation in (a)^[5] whereas bands observed at higher energies are attributed to the $\pi - \pi^*$ presenting an important percentage around 68% transitions of the phenyl rings which is consistent for polyaromatic dyes (see Table 5).^[12] It is worth mentioning that the spectrum superposition shows several absorption peaks for non-polar aprotic solvents with additional shoulders. While, If we see the absorption spectrum of both studied compounds (a) and (b) recorded in THF (Polar Solvent), a red shift is observed after complexation and the absorption spectra shows a more structured spectra presenting three relatively obvious absorption peaks ($\lambda_{abs} = 301$ nm, 369 nm and 488 nm). This is expected due to enhanced rigid structure.^[64]

After the blockage of the ESIPT core of (a) through Boron Difluoride complexation, a different scenario of absorption is observed. BF₂ moiety introduction makes all absorption spectra broader. A gradual increase of redshift is concomitantly observed for (b) from non-polar(-Cyclohexan and Toluen) to polar solvent (THF). The redshift is spanned in the range of 473 to 485 nm, 467 to 483 nm and 475 to 488 nm respectively for the experimental spectra recorded in Cyclohexan, Toluen, and THF and in the range of 461 to 484 nm (f = 0,68), 462 to 484 nm (f = 0,69) and 460 to 479 nm (f = 0,68) respectively for the theoretical spectra. Bathochromically

TABLE 5 Experimental and calculated absorption wavelength (λ_{max}), oscillatorstrengths (f) and Major and minor contributions (%) of (a) and (b) molecules using CAM-B3LYP-D3/6-311++G(d,p) level

solvents	(a)			(b)				
	λ_{Exp} (nm)	λ_{cal} (nm)	f (a.u)	Major and minor contributions (%)	λ_{Exp} (nm)	λ_{cal} (nm)	f (a.u)	Major and minor contributions (%)
Chloroform	346	340	0.261	H-2 → L + 2 (36%) H-2 → L + 1 (11%) H → L + 6 (16%)	300	334	0.442	H-1 → L + 2 (35%) H-2 → L + 1 (17%) H-1 → L + 4 (30%)
	374	377	0.265	H-2 → L (43%) H → L + 2 (38%) H → L + 1 (17%)	346	347	0.080	H-2 → L + 1 (41%) H → L + 2 (35%) H-1 → L + 2 (21%)
	418	420	0.265	H-3 → L (49%) H-1 → L (21%) H → L (10%)	389	361	0.328	H-2 → L + 1 (39%) H-4 → L (29%) H-1 → L + 1 (24%)
	485	491	0.587	H → L (68%)	409	432	0.504	H-2 → L + 2 (36%) H-2 → L + 1 (12%) H-1 → L + 4 (34%)
	---	---	---	---	477	481	0.305	H → L (69%)
Cyclohexan	363	330	0.288	H-4 → L + 2 (26%) H-2 → L + 1 (20%) H-2 → L + 2 (10%)	299	334	0.446	H-3 → L + 2 (46%) H-2 → L + 1 (32%) H-1 → L + 3 (14%)
	408	360	0.115	H → L + 2 (44%) H-4 → L (37%) H-3 → L (24%)	348	348	0.304	H-2 → L (40%) H-2 → L + 2 (18%) H-1 → L + 2 (29%)
	437	404	0.269	H-3 → L (60%) H-1 → L (14%) H-4 → L (25%)	368	362	0.319	H-3 → L (51%) H-2 → L (25%) H-1 → L + 1 (11%)
	473	461	0.487	H → L (69%)	443	432	0.486	H-2 → L + 2 (39%) H-1 → L + 1 (32%) H-1 → L + 3 (14%)
	---	---	---	---	485	484	0.313	H → L (68%)
THF	325	330	0.257	H-2 → L + 2 (36%) H-2 → L + 1 (12%) H-1 → L + 4 (34%)	301	337	0.428	H-1 → L + 1 (36%) H-2 → L + 1 (27%) H-3 → L + 2 (18%)
	345	358	0.262	H-2 → L (43%) H → L + 2 (38%) H-1 → L + 2 (18%)	347	346	0.058	H → L + 2 (24%) H-2 → L + 1 (37%) H-3 → L (25%)
	386	403	0.261	H-3 → L (49%) H-4 → L (29%)	369	360	0.325	H-3 → L (42%) H-1 → L (17%)

TABLE 5 (Continued)

solvents	(a)			(b)				
	λ_{Exp} (nm)	λ_{cal} (nm)	f (a.u)	Major and minor contributions (%)	λ_{Exp} (nm)	λ_{cal} (nm)	f (a.u)	Major and minor contributions (%)
				H-1 → L (21%) H → L (68%)	416	431	0.504	H-4 → L + 2 (23%) H-3 → L + 2 (29%) H-2 → L + 1 (24%) H-2 → L + 3 (16%)
	475	460	0.583					
	---	---	---	---	488	479	0.296	H → L (68%)
Toluene	345	330	0.216	H-2 → L + 1 (39%) H-4 → L (29%) H-1 → L + 1 (24%)	313	334	0.459	H → L + 2 (44%) H-4 → L (37%) H-3 → L (24%)
	361	360	0.260	H-1 → L + 1 (36%) H-2 → L + 1 (27%) H-3 → L + 2 (18%)	344	348	0.307	H-2 → L (43%) H → L + 2 (38%) H-1 → L + 2 (18%)
	413	403	0.272	H-3 → L + 2 (46%) H-2 → L + 1 (32%) H-1 → L + 3 (14%)	366	362	0.330	H-2 → L + 2 (36%) H-2 → L + 1 (11%) H → L + 6 (16%)
	467	462	0.587	H → L (69%)	410	432	0.498	H-2 → L (43%) H → L + 2 (38%) H → L + 1 (17%)
	---	---	---	---	483	484	0.320	H → L (69%)
Gas	---	327	0.167	H-2 → L + 1 (36%) H-2 → L + 2 (22%) H → L + 4 (15%)	---	332	0.289	H-3 → L + 2 (26%) H-2 → L + 1 (32%) H-1 → L + 3 (17%)
	---	352	0.249	H-2 → L (41%) H → L + 2 (28%) H-1 → L + 1 (113%)	---	347	0.284	H-2 → L (33%) H-2 → L + 1 (27%) H-1 → L + 2 (19%)
	---	400	0.243	H-2 → L (35%) H-1 → L (28%) H-1 → L + 1 (15%)	---	362	0.226	H-2 → L (29%) H-4 → L + 2 (24%) H-1 → L + 1 (15%)
	457	433	0.433	H → L (68%)	---	428	0.390	H-2 → L + 1 (26%) H-1 → L + 1 (32%) H-1 → L + 3 (24%)
	---	---	---	---	482	0.243	0.243	H → L (69%)

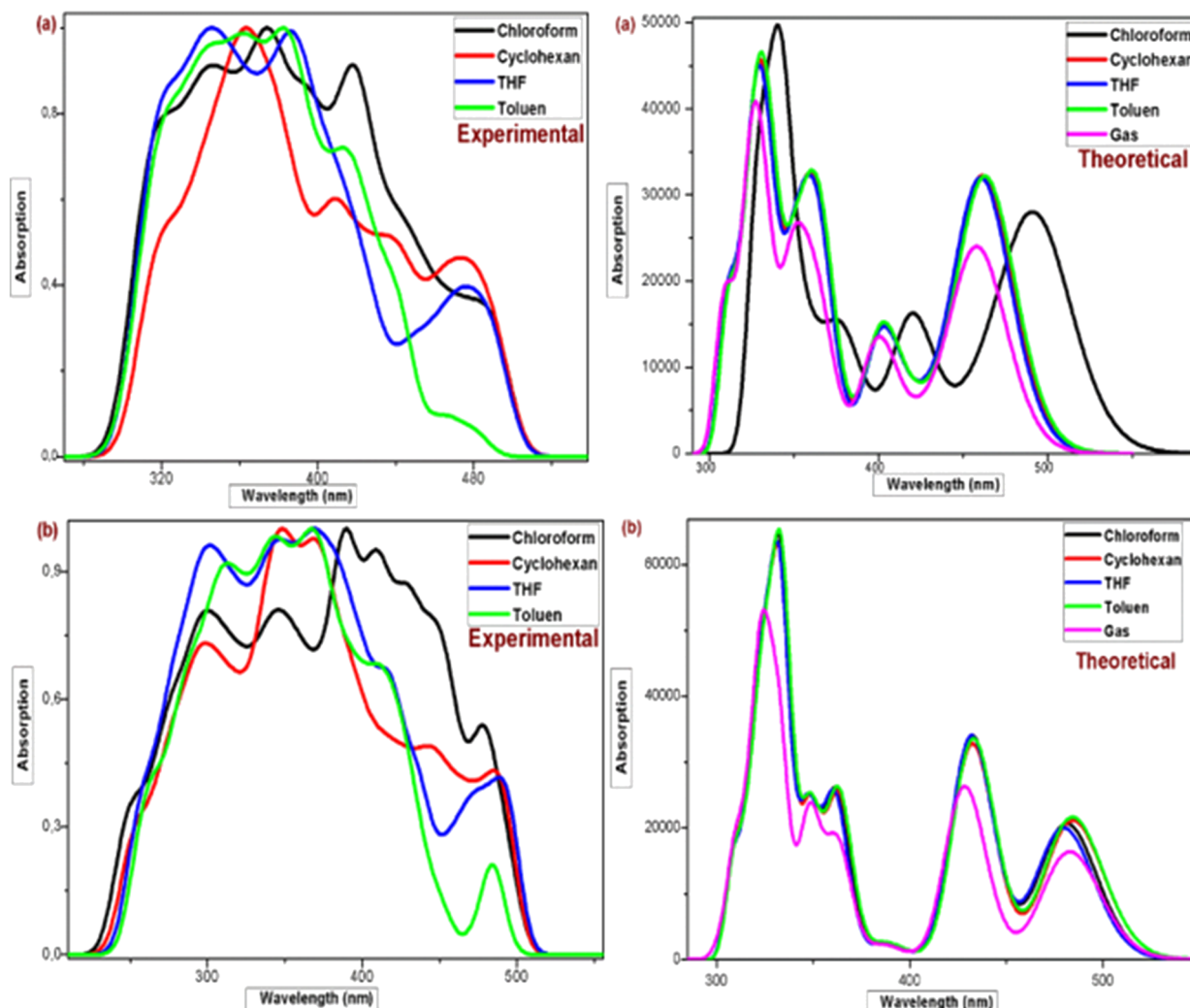


FIGURE 4 Observed and calculated UV-vis spectra of (a) and (b) in different solvents

shifted spectra have proven that both of the molecules are stabilized in each excited state. Hence it can be predicted that the studied compound is behaving like donor-acceptor compounds while the excited state of these compounds is highly stabilized in these solvents as compared to its ground state.^[65] Moreover, red shifted bands are directly related to larger electronic delocalization.^[59] It is obvious that there is a significant agreement between experimental and theoretical absorption maxima.

It is apparent, The introduction of BF₂ moiety prevents unsystematic rotations around single bonds, rigidifies the structure in addition to helping the radiative process to control the non-radiative deexcitations.^[66] The formation of the B ← N dative bond via the donation of lone-pair of the N atom to the B atom lowers the energy gap between π^* and π , which can decrease the loss of energy via vibrational motions and increases the emission efficiency.^[11] Thus, the synthesized Boranil is Blue

Fluorescent emissive in all studied solvents. Experimental Spectra of both studied compounds (a) and (b) recorded in Chloroform are superimposable. A very weak blue shift of 8 nm spanning in the range of 485–477 nm is observed in the experimental spectrum. The respective calculated spectra feature a similar blue shift of 10 nm($f = 0.68$); this means that the absorption occurs without differences in the spatial conformation of the molecules.^[66] The maximum absorption wavelength corresponds to the electronic transition from the HOMO to LUMO with a contribution of about 68–69% for both studied compounds (a) and (b) while the short wavelengths correspond to an electronic transfer between HOMO-1, HOMO-2, HOMO-3, ... to highly excited states LUMO+1, LUMO+4orbitals with moderate contributing coefficients.

To find an account, on one side, using Chloroform as a solvent gives us the predicted blue shift; on the other side spectra recorded quality is unsatisfying and not

structured in comparison with calculated spectra. From the point of view of spectra quality, peaks with several shoulders have shown a better relative response using THF. Therefore, the polarity of the solvent may be important in enhancing photophysical properties of (a) and (b) and this observation is in agreement with several recent studies.^[67]

It is clear from this investigation that the obtained experimental and theoretical spectra are in good agreement. According to Chandreskaran, the small deviation between both spectra may have resulted from the solvent effect. The solvent causes the complexation of the chemical molecular environment.^[48] The interaction between different solvents and both studied Anil and Boranil can also explain the slight fluctuations in the calculated absorption wavelength maxima.^[68]

4 | CONCLUSION

In summary, we have described the synthesis of non-substituted Anil in one step synthesis from Salicylaldehyde and Aniline followed by a Boron Difluoride complexation to form the corresponding Boranil by chelating BF_2 fragment. Subsequent investigation of Anil and Boranil optical properties has shown that the Boranil dye displays sizable emission property in all studied solvents. Once the possibility of Anil tautomerization is removed by replacement of the OH proton by BF_2 , the comparison of different modes in NMR signals and IR spectra proves the successful structural modification.

Observed Redshift for most of studied solvents is an evident proof for charge transfer interaction between the donor (phenyl rings) and the acceptor group (BF_2 moiety) through the delocalization of π system. This along with the lowering of HOMO-LUMO band gap and destabilizing the molecule's ground state. The redshift is observed in THF (polar solvent), Cyclohexan and Toluenspectra. Meanwhile, the expected blueshift is only observed in the absorption spectra recorded in Chloroform. The complicated photophysics of Anil is the result of many possible processes that can occur with important rates in the excited molecule such as proton transfer and free rotation occurring in solution. Our results efficaciously allow suppressing these processes by a judicious choice of solvent and different complexation factors. All calculated findings are in excellent agreement with experimental data. We hope that the present results will contribute to a deeper understanding of the synthesis protocols and photophysics of Anils and Boranils. We expect that the new Boranil complexe reported here will have potential applications in Bio-imaging applications since emission properties in solution are not affected by

media polarities. Current studies on the modification of conjugated Fluorescent systems and emission properties are in progress.

ACKNOWLEDGMENTS

The authors greatly acknowledge financial support between cooperation Tunisia-Morocco for funding the work through the research program N°17/TM10.

CONFLICT OF INTEREST

The authors declare that they have no conflict of interest.

ORCID

Abdul-Rahman Allouche  <https://orcid.org/0000-0003-0725-4057>
Mohamed Hassen V Baouab  <https://orcid.org/0000-0003-2069-7151>

REFERENCES

- [1] S. Chen, R. Qiu, Q. Yu, X. Zhang, M. Wei, Z. Dai, *Tetrahedron Lett.* **2018**, *59*, 2671.
- [2] M. M. Corona-López, V. M. Jiménez Pérez, R. Chan-Navarro, M. Ibarra-Rodríguez, H. V. Rasika Dias, A. Chávez-Reyes, B. M. Muñoz-Flores, *J. Organomet. Chem.* **2017**, *852*, 64.
- [3] Y. Liu, Q. Bai, J. Li, S. Zhang, C. Zhang, F. Lu, B. Yang, P. Lu, *RSC Adv.* **2016**, *6*, 17239.
- [4] T. Shan, Y. Liu, X. Tang, Q. Bai, Y. Gao, Z. Gao, J. Li, J. Deng, B. Yang, P. Lu, Y. Ma, *ACS Appl. Mater. Interfaces* **2016**, *8*, 28771.
- [5] Y. Zhang, S.-L. Lai, Q.-X. Tong, M.-F. Lo, T.-W. Ng, M.-Y. Chan, Z.-C. Wen, J. He, K.-S. Jeff, X.-L. Tang, W.-M. Liu, C.-C. Ko, P.-F. Wang, C.-S. Lee, *Chem. Mater.* **2012**, *24*, 61.
- [6] D. Kumar, K. R. Justin Thomas, C.-P. Lee, K.-C. Ho, *J. Org. Chem.* **2014**, *79*, 3159.
- [7] B. Umamahesh, J. Ajantha, C. Sravani, S. Easwaramoorthi, K. I. Sathiyaranayanan, *Dyes Pigm.* **2017**, *137*, 182.
- [8] J. Zhai, T. Pan, J. Zhu, Y. Xu, J. Chen, Y. Xie, Y. Qin, *Anal. Chem.* **2012**, *84*, 10214.
- [9] K. Dhananjayarao, V. Mukundam, K. Venkatasubbaiah, *Inorg. Chem.* **2016**, *55*, 11153.
- [10] K. Zhang, H. Zheng, C. Hua, M. Xin, J. Gao, Y. Li, *Tetrahedron* **2018**, *74*, 4161.
- [11] A. Kilic, F. Alcay, M. Aydemir, M. Durgun, A. Keles, A. Baysal, *Spectrochim. Acta, Part A* **2015**, *142*, 62.
- [12] D. Frath, K. Benelhadj, M. Munch, J. Massue, G. Ulrich, *J. Org. Chem.* **2016**, *81*, 9658.
- [13] H. Doušová, P. Šimůnek, N. Almonasy, Z. Růžičková, *J. Organomet. Chem.* **2016**, *802*, 60.
- [14] A. Kilic, M. Aydemir, M. Durgun, N. Meriç, Y. S. Ocak, A. Keles, H. Temel, *J. Fluorine Chem.* **2014**, *162*, 9.
- [15] K. Dhananjayarao, V. Mukundam, M. Ramesh, K. Venkatasubbaiah, *Eur. J. Inorg. Chem.* **2014**, *2014*, 539.
- [16] M. Urban, K. Durka, P. Jankowski, J. Serwatowski, S. Luliński, *J. Org. Chem.* **2017**, *82*, 8234.
- [17] K. Kamada, T. Namikawa, S. Senatore, C. Matthews, P.-F. Lenne, O. Maury, C. Andraud, M. Ponce-Vargas, B. Le

- Guennic, D. Jacquemin, P. Agbo, D. D. An, S. S. Gauny, X. Liu, R. J. Abergel, F. Fages, A. D'Aléo, *Chem. – Eur. J.* **2016**, *22*, 5219.
- [18] E. Dai, W. Pang, X.-F. Zhang, X. Yang, T. Jiang, P. Zhang, C. Yu, E. Hao, Y. Wei, X. Mu, L. Jiao, *Chem. – Asian J.* **2015**, *10*, 1327.
- [19] S. Yamaguchi, A. Wakamiya, *Pure Appl. Chem.* **2006**, *78*, 1413.
- [20] M. Graser, H. Kopacka, K. Wurst, M. Ruetz, C. R. Kreutz, T. Müller, C. Hirtenlehner, U. Monkowius, G. Knör, B. Bildstein, *Inorg. Chim. Acta* **2013**, *405*, 116.
- [21] D. Frath, S. Azizi, G. Ulrich, P. Retailleau, R. Ziessel, *Org. Lett.* **2011**, *13*, 3414.
- [22] D. Frath, S. Azizi, G. Ulrich, R. Ziessel, *Org. Lett.* **2012**, *14*, 4774.
- [23] G. Wesela-Bauman, M. Urban, S. Luliński, J. Serwatowski, K. Woźniak, *Org. Biomol. Chem.* **2015**, *13*, 3268.
- [24] Y.-L. Rao, S. Wang, *Organometallics* **2011**, *30*, 4453.
- [25] M. Chaabene, S. Agren, A.-R. Allouche, M. Laheinie, R. B. Chaâbane, M. H. V. Baouab, *Appl. Organomet. Chem.* **2019**, *33*, e5218.
- [26] J. Dobkowski, P. Wnuk, J. Buczyńska, M. Pszona, G. Orzanowska, D. Frath, G. Ulrich, J. Massue, S. Mosquera-Vázquez, E. Vauthey, C. Radzewicz, R. Ziessel, J. Waluk, *Chem. – Eur. J.* **2015**, *21*, 1312.
- [27] J. M. Ortiz-Sánchez, R. Gelabert, M. Moreno, J. M. Lluch, *J. Phys. Chem. A* **2006**, *110*, 4649.
- [28] L. Hu, J. Pan, X. Zhang, W. Hu, Y. Xiong, X. Zhu, *Tetrahedron* **2017**, *73*, 223.
- [29] S. Grimme, J. Antony, S. Ehrlich, H. Krieg, *J. Chem. Phys.* **2010**, *132*, 154104.
- [30] A. D. Becke, *Phys. Rev. a* **1988**, *38*, 3098.
- [31] C. Lee, W. Yang, R. G. Parr, *Phys. Rev. B* **1988**, *37*, 785.
- [32] R. Ditchfield, *J. Chem. Phys.* **1972**, *56*, 5688.
- [33] K. Wolinski, J. F. Hinton, P. Pulay, *J. Am. Chem. Soc.* **1990**, *112*, 8251.
- [34] N. M. O'boyle, A. L. Tenderholt, K. M. Langner, *J. Comput. Chem.* **2008**, *29*, 839.
- [35] R. Bauernschmitt, R. Ahlrichs, *Chem. Phys. Lett.* **1996**, *256*, 454.
- [36] M. E. Casida, C. Jamorski, K. C. Casida, D. R. Salahub, *J. Chem. Phys.* **1998**, *108*, 4439.
- [37] M. J. Frisch, G. W. Trucks, H. B. Schlegel, G. E. Scuseria, M. A. Robb, J. R. Cheeseman, G. Scalmani, V. Barone, G. A. Petersson, H. Nakatsuji, X. Li, M. Caricato, A. Marenich, J. Bloino, B. G. Janesko, R. Gomperts, B. Mennucci, H. P. Hratchian, J. V. Ortiz, A. F. Izmaylov, J. L. Sonnenberg, D. Williams-Young, F. Ding, F. Lipparini, F. Egidi, J. Goings, B. Peng, A. Petrone, T. Henderson, D. Ranasinghe, V. G. Zakrzewski, J. Gao, N. Rega, G. Zheng, W. Liang, M. Hada, M. Ehara, K. Toyota, R. Fukuda, J. Hasegawa, M. Ishida, T. Nakajima, Y. Honda, O. Kitao, H. Nakai, T. Vreven, K. Throssell, J. A. Montgomery Jr., J. E. Peralta, F. Ogliaro, M. Bearpark, J. J. Heyd, E. Brothers, K. N. Kudin, V. N. Staroverov, T. Keith, R. Kobayashi, J. Normand, K. Raghavachari, A. Rendell, J. C. Burant, S. S. Iyengar, J. Tomasi, M. Cossi, J. M. Millam, M. Klene, C. Adamo, R. Cammi, J. W. Ochterski, R. L. Martin, K. Morokuma, O. Farkas, J. B. Foresman, D. J. Fox, Gaussian 09, Revision A.02, Gaussian, Inc., Wallingford CT, **2016**.
- [38] A.-R. Allouche, *J. Comput. Chem.* **2011**, *32*, 174.
- [39] V. Arjunan, M. Kalaivani, M. K. Marchewka, S. Mohan, *J. Mol. Struct.* **2013**, *1045*, 160.
- [40] H. Zhang, C. Liu, *Dyes Pigm.* **2017**, *143*, 143.
- [41] K. Dhanunjayarao, V. Mukundam, K. Venkatasubbaiah, *J. Mater. Chem. C* **2014**, *2*, 8599.
- [42] F. P. Macedo, C. Gwengo, S. V. Lindeman, M. D. Smith, J. R. Gardiner, *Eur. J. Inorg. Chem.* **2008**, *2008*, 3200.
- [43] Q.-C. Yao, D.-E. Wu, R.-Z. Ma, M. Xia, *J. Organomet. Chem.* **2013**, *743*, 1.
- [44] M. A. Ashraf, K. Mahmood, A. Wajid, I. B. Yusoff, *Synthesis, Characterization and Biological Activity of Schiff Bases*, IACSIT Press, Singapore **2011**.
- [45] H. Ünver, K. Polat, M. Uçar, D. M. Zengin, *Spectrosc. Lett.* **2003**, *36*, 287.
- [46] R. M. Issa, A. M. Khedr, H. Rizk, *J. Chin. Chem. Soc.* **2008**, *55*, 875.
- [47] N. N. Shapetko, L. N. Kurkovskaya, V. G. Medvedeva, A. P. Skoldinov, L. K. Vasyanina, *J. Struct. Chem.* **1970**, *10*, 824.
- [48] K. Chandrasekaran, R. Thilak Kumar, *Spectrochim. Acta, Part A* **2015**, *150*, 974.
- [49] K. Benelhadj, J. Massue, P. Retailleau, G. Ulrich, R. Ziessel, *Org. Lett.* **2013**, *15*, 2918.
- [50] NIST Computational Chemistry Comparison and Benchmark Database, NIST Standard Reference Database Number 101, Release 19, April **2018**, Editor: Russell D. Johnson III, <http://cccbdb.nist.gov/>.
- [51] H. Nakano, T. Inoue, N. Kawasaki, H. Miyataka, H. Matsumoto, T. Taguchi, N. Inagaki, H. Nagai, T. Satoh, *Bioorg. Med. Chem.* **2000**, *8*, 373.
- [52] K. B. Benzon, H. T. Varghese, C. Y. Panicker, K. Pradhan, B. K. Tiwary, A. K. Nanda, C. V. Alsenoy, *Spectrochim. Acta, Part A* **2015**, *146*, 307.
- [53] A. Suvitha, S. Periandy, P. Gayathri, *Spectrochim. Acta, Part A* **2015**, *138*, 357.
- [54] N. Prabavathi, A. Nilufer, V. Krishnakumar, *Spectrochim. Acta, Part a* **2012**, *92*, 325.
- [55] T. Rajamani, S. Muthu, *Solid State Sci.* **2013**, *16*, 90.
- [56] M. Chaabene, B. Gassoumi, P. Mignon, R. Ben Chaâbane, A.-R. Allouche, *J. Mol. Graphics Modell.* **2019**, *88*, 174.
- [57] R. Soury, M. Chaabene, M. Jabli, T. A. Saleh, R. Ben Chaabane, E. Saint-Aman, F. Loiseau, C. Philouze, A.-R. Allouche, H. Nasri, *Chem. Eng. J.* **2019**, *375*, 122005.
- [58] M. Arivazhagan, S. Prabhakaran, R. Gayathri, *Spectrochim. Acta, Part A* **2011**, *82*, 332.
- [59] R. Chan-Navarro, V. M. Jiménez-Pérez, B. M. Muñoz-Flores, H. V. R. Dias, I. Moggio, E. Arias, G. Ramos-Ortíz, R. Santillan, C. García, M. E. Ochoa, M. Yousufuddin, N. Waksman, *Dyes Pigm.* **2013**, *99*, 1036.
- [60] A. Mohamadi, M. Shabanian, M. Hajibeygi, H. Moghanian, *J. Chil. Chem. Soc.* **2013**, *58*, 1659.
- [61] S. Park, J. E. Kwon, S. Y. Park, *Phys. Chem. Chem. Phys.* **2012**, *14*, 8878.
- [62] S. Kothavale, N. Sekar, *ChemistrySelect* **2017**, *2*, 7691.
- [63] B. M. Muñoz, R. Santillan, M. Rodríguez, J. M. Méndez, M. Romero, N. Farfán, P. G. Lacroix, K. Nakatani, G. Ramos-Ortíz, J. L. Maldonado, *J. Organomet. Chem.* **2008**, *693*, 1321.

- [64] J.-W. Hu, H.-Y. Tsai, S.-K. Fang, C.-W. Chang, L.-C. Wang, K.-Y. Chen, *Dyes Pigm.* **2017**, *145*, 493.
- [65] S. Somasundaram, E. Kamaraj, S. J. Hwang, S. Park, *Spectrochim. Acta, Part A* **2018**, *191*, 325.
- [66] B. Jędrzejewska, A. Zakrzewska, G. Młostoni, Š. Budzák, K. Mroczynska, A. M. Grabarz, M. A. Kaczorowska, D. Jacquemin, B. Ośmiałowski, *J. Phys. Chem. A* **2016**, *120*, 4116.
- [67] V. S. Padalkar, S. Seki, *Chem. Soc. Rev.* **2016**, *45*, 169.
- [68] N. S. Bayliss, *J. Chem. Phys.* **1950**, *18*, 292.

How to cite this article: Agren S, Chaabene M, Allouche A-R, Ben Chaâbane R, Lahcinie M, Baouab MHV. Blue Highly Fluorescent Boranil Derived From Anil Ligand: Synthesis, Characterization, Experimental and Theoretical Evaluation of Solvent Effect on Structures and Photophysical Properties. *Appl Organomet Chem.* 2020;e5764. <https://doi.org/10.1002/aoc.5764>